This article has been accepted for inclusion in a future issue of this journal. Content is final as presented, with the exception of pagination.

SXR Measurements in INTI PF Operated in Neon to Identify Typical (Normal N) Profile for Shots With Good Yield

Sor Heoh Saw, Rajdeep Singh Rawat, Paul Lee, Alireza Talebitaher, Ali E. Abdou, Perk Lin Chong, Federico Roy, Jr, *Member, IEEE*, Jalil Ali, and Sing Lee

***Abstract*— The six-phase Lee model code was developed to compute the anomalous resistance phase (RAN) following the pinch phase in a plasma focus (PF) discharge. One important method to check such modeling is to look at the soft X-ray (SXR) emission time profile and to correlate this to the PF dynamics. A two-channel filtered SXR spectrometer coupled with an Excel-based analytical template was recently developed to speed up the correlation process. Using this system, we have determined that the neon PF typically operates in a normal (N) mode in which it emits characteristic He-like H-like neon line SXR (in a photon energy window of 900–1550 eV) reproducibly and efficiently. The characteristic neon line SXR pulse straddles the pinch duration starting strongly 10 ns before the start of the pinch, then diminishes through the 10-ns pinch and tails off into the subsequent RAN1 phase. We present the correlated time profiles of shots operating in the efficient N mode as well as, for comparison, poor shots, which are distinctly different in SXR time profiles. The profiles indicate the difference in dynamics of normal and poor shots. Statistics are presented as well as comparison of the yields from the numerical experiments and measurements. In the series that were studied the proportion of N-mode operation ranges from 70% in one series to 80% in another series over pressure range 1–4 torr. At 2 torr, it was found that 90% recorded the normal N profile. The results reinforce the view that while the Lee Model code incorporates the correct physics in its sequence of phases, refinement is needed to extend the radiative phase to the period before the pinch.**

***Index Terms*— Neon soft X-rays (SXRs), plasma focus (PF), plasma focus (PF) modeling, soft X-ray (SXR) measurements.**

Manuscript received April 6, 2013; revised June 2, 2013; accepted September 4, 2013.

S. H. Saw is with the INTI International University, Nilai 71800, Malaysia, and also with the Institute for Plasma Focus Studies, Melbourne 3148, Australia (e-mail: sorheoh.saw@newinti.edu.my).

R. S. Rawat, P. Lee, and A. Talebitaher are with the Nanyang Technological University, National Institute of Education, Singapore 637616 (e-mail: rajdeep.rawat@nie.edu.sg; paul.lee@nie.edu.sg; alireza.talebitaher@nie.edu.sg).

A. E. Abdou was with the Department of Mechanical and Nuclear Engineering, Kansas State University, Manhattan, KS 66506 USA. He is now with the Zewail City of Science and Technology, Cairo 12588, Egypt (e-mail: aeabdou@ksu.edu).

P. L. Chong and F. Roy are with INTI International University, Nilai 71800, Malaysia (e-mail: perklin.chong@newinti.edu.my; federico.royjr@newinti.edu.my).

J. Ali is with the Institute of Advanced Photonic Science, Nanotechnology Research Alliance, Universiti Teknologi Malaysia, Johor Baru 81310, Malaysia (e-mail: jalilali@utm.edu.my).

S. Lee is with INTI International University, Malaysia, and also with the Institute for Plasma Focus Studies, Melbourne 3148, Australia, and also with the University of Malaya, Kuala Lumpur 50603, Malaysia (e-mail: leesing@optusnet.com.au).

Color versions of one or more of the figures in this paper are available online at http://ieeexplore.ieee.org.

Digital Object Identifier 10.1109/TPS.2013.2281333

I. Introduction

The dynamics of the plasma focus (PF) computed from the Lee model code is found to be in general agreement with the experimental measurements when the computed current waveform is properly fitted to the measured current waveform [1]–[11]. The features in agreement include the temporal profiles of the axial and the radial speeds.

Recently, it was found [12] that PF devices need to be classified into T1 and T2 the former having low static inductance L_0 typically in the tens of nanohenries (nH) while the latter typically have L_0 of 100 nH or more. To complete the fit for T2 devices the five-phase Lee Model code was extended to the six-phase code with the addition of a postpinch phase of anomalous resistance. With this new six-phase code, the computed current waveform is fitted very well to the measured current waveform.

The neon PF produces He-like H-like neon line soft X-ray (SXR) (termed as characteristic neon SXR) at a pinch plasma temperature of 200–500 eV in a spectral range 8–13.5-Å (photon energy window of 900–1550 eV) [3], [7], [13]. In an earlier paper, we had already shown the correlation between the temporal history of the measured SXR pulse with different phases of the computed current waveform, which has been fitted to the measured current waveform [13]. In this paper, we present the comparative time profiles for typical normal (N) shots in which the plasma focuses efficiently and reproducibly. We also present the time profiles of the nonnormal shots, which are termed as poor being invariably erratic and inefficient in characteristic neon SXR yield. The comparison enables us to draw the conclusions regarding the dynamics and statistics of good and bad shots. This could prove important for the development of the PF as SXR sources.

II. Method

A. Experiment

The experiments are carried out using the INTI PF, which is one of the machines in the network of United Nations University/ International Centre for Theoretical Physics Plasma Focus Facility's [14]. The INTI PF had its electrical parameters determined as follows: static inductance $L_0 = 114$ nH, capacitance $C_0 = 30\ \mu$F, and bank stray resistance $r_0 = 13$ mΩ; its tube parameters are: cathode radius $b = 3.2$ cm, anode radius $a = 0.95$ cm, and anode length $z_0 = 16$ cm. The pressure range covered in these experiments was 1.1–4.3 torr at 12 kV. X-ray (XR) pulses (from two detector channels of diode X-ray spectrometer), the measured rate of change of current dI/dt and the tube voltage are recorded together on a four-channel digital storage oscilloscope. The voltage signal is obtained using a resistive divider with a time response in the region of 15 ns [14]. The dI/dt signal is from a seven-turn Rogowski coil wrapped around one of the 16 conductors returning the current from the focus tube to the capacitor earth [15].

The absorption filters method based on foil absorbers and silicon p-i-n diode detectors is used in the SXR spectrometer [16]. The two SXR detectors are used together as a differentially filtered pair, Ch1 and Ch2, to measure the characteristic He-like and H-like neon line SXR by the method of subtraction [17]. Each detector consists of a reverse-biased windowless BXP65 p-i-n photodiode with a wide spectral range.

In designing the required filter, the emission wavelength with expected line intensities are suitably weighted and factored in [18] and [19] to obtain the average sensitivity factor for the desired relatively narrow spectral window of 900–1550 eV. The first detector is covered with 13 μm Al (XR Al Ch1). The second detector is covered with 3-μm Al+125-μm Mylar (XR Mylar Ch2).

Factoring in the quantum detection efficiency [20] of silicon, XR transmission efficiency through neon gas at different pressure and fixed path length of 25 cm between the anode tip and the detector; and the XR attenuation length of solids [21], the two sensitivity curves are identical and appear as one curve, except for a sharp spike on the left side of the curve with photonic energy range 900–1550 eV. This spike (transmission window) belongs to Ch1 only. Thus, the difference pulse obtained by subtracting Ch2 pulse from Ch1 pulse is a pulse of radiation having photonic energy range 900–1550 eV. Any difference pulse is due to neon characteristic SXR while pulses with identical Ch1 and Ch2 magnitudes (thus, with no difference pulse) is due to radiation other than neon characteristic lines and is likely due to radiation harder than 1550 eV. This method had been discussed in detail in [13].

With this sensitivity curve, the absolute amount of characteristic neon line SXR falling on the detector is measured; and the source yield estimated by space integrating over 4π; and time integrating over the duration of the pulse. Both detectors have been normalized to one another and are positioned side by side with the same distance to the focus position where the focus pinch emits the radiation to be detected.

B. Numerical Experiment

The parameters of the INTI PF, as listed above were determined [22] and the code [1] is configured accordingly.

The computed current is fitted to the measured current [1]–[11] by varying the mass factor f_m and the current factor f_c for the axial phase; then the radial parameters f_{mr} and f_{cr} for the radial phase and finally the anomalous resistance parameters (amplitude of resistance, rise time, and fall time for up to three sequential anomalous resistances). The critical topping region is expanded again and again as the fitting is fine-tuned until an accuracy of 2–4 ns is typically achieved in the fitting of the computed to the measured current waveforms, particularly at the roll-over region where the apparent beginning of the dip occurs. From the experience, we know that the end of the axial phase actually occurs a little before this roll-over starts to become apparent.

The end result is the computed current waveform is fitted so well to the measured current waveform that the two curves overlap each other over the whole range of fitting (see Fig. 1) at the level of time magnification to a resolution of 2–4 ns. The dynamics of the discharge is obtained from the computation. Since the computed current waveform is correctly fitted to the measured waveform, the computed energetics matches that of the actual discharge. In that sense, the computed dynamics is considered as a realistic representation of the actual dynamics of the actual shot. From the computed dynamics, we obtain the time of the start of the radial phase and the times of start and end of the pinch phase. These are correlated to the XR pulses.

C. Correlating the Time History

An analytical template was designed in the form of an Excel Workbook with four work sheets [1]. Sheet 1 is the numerical experiment RADPFV6.1b, which runs numerical experiments configured as a specific PF. Sheet 2 extends Sheet 1 with more detailed presentation of the results of Sheet 1 in terms of PF dynamics, energy distributions, and plasma properties. Sheet 4 contains the measured data of the experiment with tube voltage, SXR Al filtered (Ch1), SXR Mylar filtered (Ch2), and rate of change of current.

The numerical results of Sheet 1 and the measured data of Sheet 4 are correlated in Sheet 3. The correlation results are shown (for example each of the six figures in Fig. 1 shows the correlation of a shot) and discussed in this paper.

III. Results

A. First Series

For ease of comparison of time profiles, the correlation images in Fig. 1 have been adjusted to have the same time scale and amplitude scale and are all aligned at the start of the radial phase (the single dashed vertical line on the left side of each image). A series of 21 shots in neon at 12 kV and pressure in the range 1.1–4.3 torr was analyzed and six representative shots are shown in Fig. 1(a)–(f). The key to these figures are shown in Table I.

Fig. 1(a) shows the correlation of the first shot of the series that is considered as a conditioning shot, which removes gases that are adsorbed into the electrodes during the days of inactivity of the PF before the present series. If the PF electrodes are kept at a pressure not exceeding a few torrs and are not exposed to the atmosphere, then typically one or two conditioning shots are sufficient to bring the plasma focus to efficient operation. During the first conditioning shot at 2 torr, as shown in Fig. 1(a), the radial phase starts relatively late at 3.7 μs from the start of current; whereas after conditioning; for a shot at 2 torr, the radial phase would start at 3.4–3.5 μs. This delayed start of the radial phase is confirmed in Fig. 2(a), also a conditioning shot of another series. The comparison of Figs. 1(a) and 2(a) shows that in both the conditioning shots only XR Al Ch 1 records weak pulses, coming before the start of pinch; and in the case of Fig. 1(a), XR Al Ch1 records

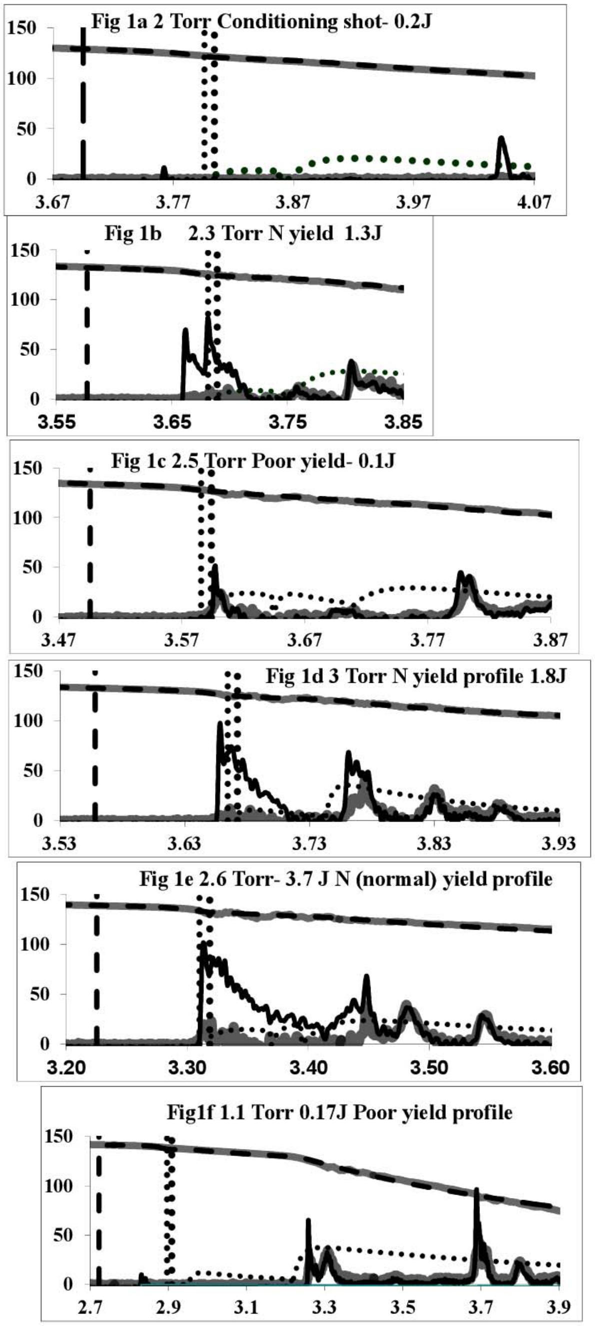

Fig. 1. First series: Correlation of characteristic neon SXR pulses with dynamics, showing typical conditioning, good focus (N profile), and bad focus shots. Each figure shows the profiles during the current dip on a time scale so highly magnified that the current dip appears as a rather gentle decline with time. The vertical scale is in kiloampere for the current traces, arbitrary scale for the XR, and anomalous resistance. The horizontal scale is in μs timed from the start of current. For comparison, the figures are aligned at the start of the radial phase (vertical dashed line on left side of each figure). The key to this figure is shown in Table I. The computed current trace overlaps the measured, the two appearing as one. For good shots (N profile: e.g., 1b, d, and e) XR Al Ch1 pulse (darker thinner line) typically has a first pulse higher than XR Mylar Ch2 pulse (lighter thicker line) but subsequently the two pulses merge as one toward the end of the second pulse and remain practically inseparable beyond.

a small second pulse that occurs some 300 ns after the pinch. XR Mylar Ch 2 records almost no signal. Hence, the weak XR pulses of the conditioning shots are characteristic neon SXRs.

TABLE I

KEY TO THE FIGS. 1 AND 2: MEASURED CURRENT, FITTED COMPUTED CURRENT, FITTED ANOMALOUS RESISTANCE, XR PULSE FROM Ch 2 WITH 125 μm MYLAR FILTER, XR PULSE FROM Ch1 WITH 13 μm Al FILTER; VERTICAL DASHED LINE MARKS TIME OF START OF RADIAL PHASE AND TWO DOTTED VERTICAL LINES MARK THE TIME OF START AND TIME OF END OF RADIAL PINCH PHASE

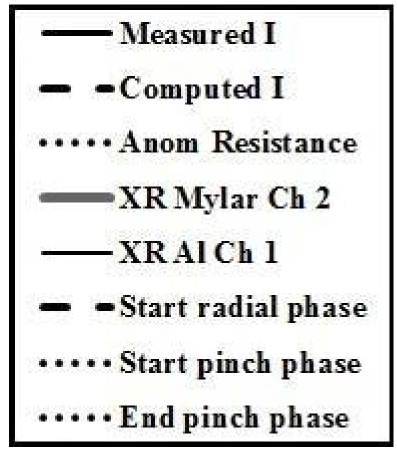

Note that in Figs. 1(a) and 2(a) only one XR (Ch1) trace is observed, the other XR trace (Ch2) is so close to the baseline that the trace does not show. Where both XR traces are of different amplitudes [see Fig. 1(d) first pulse and first part of second pulse] both the traces are clearly observed. Where both XR traces are of the same amplitude [see Fig. 1(d) falling edge of second pulse and all of the third and succeeding pulses] the overlapping of the two traces produce one thickened trace.

Fig. 1(b), (d), and (e) records typical efficient (normal) focus discharges generating good characteristic neon SXR yields. The first XR pulse is predominantly characteristic neon SXR with large XR Al Ch1 pulse and XR Mylar Ch2 pulse practically absent, the line appearing close to the baseline [Fig. 2(b), (c), (e), and (f) in series 2 also show this feature]. The difference pulse (subtracting XR Mylar Ch 2 from XR Al Ch 1) starts at or just before the pinch, continues through the pinch, and then decays after the pinch. The first pulse of SXR is followed 100 ns later by a second pulse, which starts off with a difference pulse [Figs. 1(d) and (e) and 2(c) and (e)] for a small part of the second pulse; for the rest of the second pulse XR Mylar Ch2 signal become as big as the XR Al Ch1 pulse so that there is no difference pulse. Thus, most of the characteristic neon SXR are produced in the first pulse (20–40 ns) straddling the pinch. Fig. 1(b) looks a little different from the others in that its difference pulse starts a little earlier (relative to the pinch) and appears to have a more prominent double-pulse feature than the others.

The shots with the largest yields (2–3 J) all start a few nanoseconds before the pinch, continue through the pinch and continue to produce difference pulse for a longer period than the other shots.

B. Statistics of Normal Shots

For series 1, despite the wide range of pressures 1.1–3 torr, 13 shots were identified as having SXR pulse histories

This article has been accepted for inclusion in a future issue of this journal. Content is final as presented, with the exception of pagination.

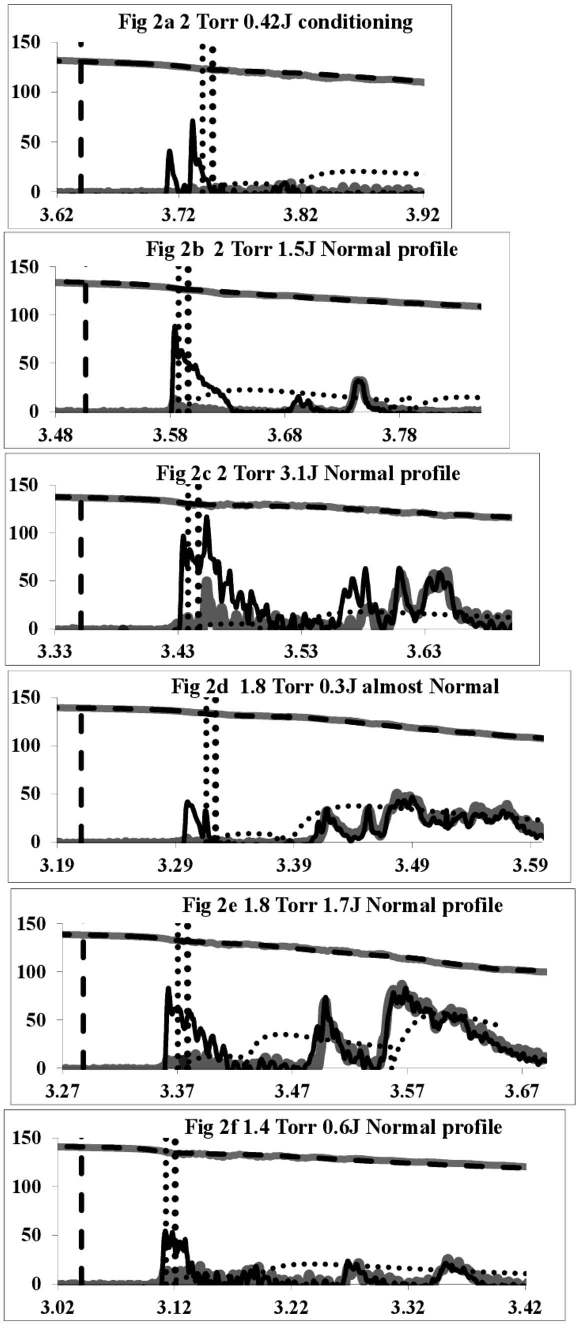

Fig. 2. Second series: Correlation of characteristic neon SXR pulses with dynamics, showing conditioning, good focus, and bad focus shots. Each figure shows the profiles during the current dip on a time scale so highly magnified that the current dip appears as a rather gentle decline with time. The vertical scale is in kiloampere for the current traces, arbitrary scale for the XR, and anomalous resistance. The horizontal scale is in μs timed from the start of current. For comparison, the figures are aligned at the start of the radial phase (vertical dashed line on left side of each figure). As in Fig 1, it is found that for good shots (N profile: e.g., 1b, d, and e) XR Al Ch1 pulse (darker thinner line) typically has a first pulse higher than XR Mylar Ch2 pulse (lighter thicker line) but subsequently the two pulses merge as one toward the end of the second pulse and remain practically inseparable beyond.

of a distinctive type, which we classify as Normal or N. These N shots have a prominent first pulse, which emits the bulk of the characteristic neon line SXR of the entire pulse chain. This first pulse correlates with the computed pinch phase; the characteristic neon SXR pulse typically starting either at the start of the pinch, or just before the pinch. In either case, this first pulse goes through the whole pinch phase and extends into the first anomalous resistance phase typically with decreasing amplitude. This first pulse, which has a half-width typically in the range 20–40 ns is followed by two to three similar shaped pulses, which carry a very little characteristic neon line SXR. The whole train of pulses typically spans 200–300 ns. These subsequent SXR pulses probably emit mainly Bremsstrahlung [23] from fully ionized neon due to an increased temperature from the anomalous resistance. Moreover, whenever these common features are observed, the characteristic neon line SXR yield over the pressure range 1.6–3.5 torr is in the range 1–4 J. The nonN shots have yields of characteristic neon line SXR significantly below this range of N yields.

Discounting the conditioning shots, then the 13 N shots represent 70% of the series. The observation that efficient emission of characteristic neon line SXR occurs whenever the measured first SXR pulse coincides with the computed pinch shows that the model does simulate the physical reality reasonably well at least in terms of the sequence of events. These observations justify designating these shots as normal (N).

C. Second Series

A second series from 1.4 to 2 torr in Neon at 12 kV was run to confirm the above identification of the N shot. Results from the earlier work had indicated that 2 torr is an operating point of good reproducibility and good yield. Therefore, we tested six shots operated at 2 torr in addition to the first conditioning shot. All these six shots produce efficient normal N profiles, representatives of which are shown in Fig. 2(b) and (c). In Fig. 2(b), the first XR pulse shows all the features of the normal N profile with the first pulse straddling the computed pinch phase. During this first XR pulse, the amplitude of Ch1 far exceeds that of Ch2; so this pulse consists of characteristic neon SXR. The second relatively small pulse is also mainly characteristic neon SXR while the third pulse consists of harder XRs. This is very similar to Fig. 1(d) and (e). Fig. 2(c) has similar characteristics but has a bigger neon SXR yield when compared with Fig. 2(b); the increased yield is due mainly to bigger width of the first pulse. Fig. 2(e) at 1.8 torr is also normal although the second pulse has a little characteristic neon SXR. We also show Fig. 2(f) at 1.4 torr, which shows a similar normal characteristic for the first pulse but again has practically no neon SXR subsequently. Comparing the pulses as a sequence it appears that below 2 torr, the subsequent pulses (after the first pulse) contributes less and less to the characteristic neon SXR as the pressure is reduced. Fig. 2(d) shows a poor shot at 1.8 torr [compared with Fig. 2(e)]. The neon characteristic SXR pulse appears to come a little earlier than normal (by 10 ns) with a very small amplitude and duration.

Discounting the conditioning shot, we have 13 out of 17 (77%) shots in this series identified as N. The characteristic neon line SXR yield for these N shots is in the range 0.5–3 J over the range of pressures. All the six shots at 2 torr are N shots with yields in the range 1.5–3 J.

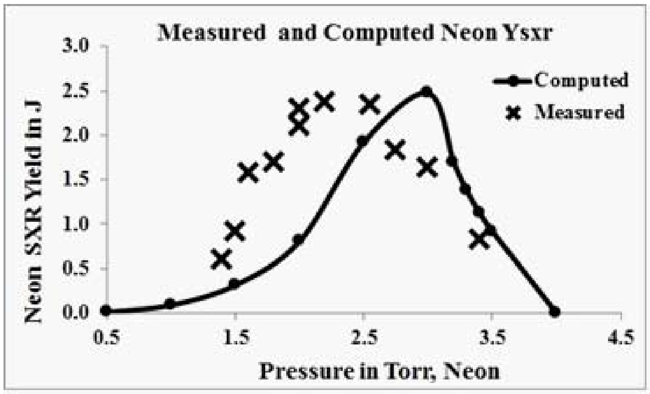

Fig. 3. Comparison of measured and computed characteristic neon SXR yield.

Considering the two series together we now present Figs. 1(b), (d), and (e) and 2(b), (c), (e), and (f) as having the efficient normal N profile. Shot 2f is included although it yields a low 0.6 J. The low yield is due to this shot being operated at the lowest pressure of the series. The rest of the shots shown in the Figs. 1 and 2 are either conditioning or poor shots and do not have the N profile. Considering all the shots of the two series, the shots having an efficient N profiles comprise 75% of all the shots, not counting the three conditioning shots. Moreover, 90% of the nonconditioning 2-torr shots exhibit the efficient N profile.

D. Yield Versus Pressure

As a further test of the validity of the modeling, we compile the measured yield (averaged at each pressure) versus pressure data and compare with the computed yield versus pressure in Fig. 3. Fig. 3 combines the results of 66 shots with 12 shots taken between 3 and 3.5 torr, 12 shots between 2.5 and 2.9 torr, eight shots between 2.1 and 2.3 torr, 18 shots at 2 torr, 16 shots between 1.4 and 1.8 torr. We found that operation at 2 torr produce the best consistency, with 90% of the shots showing N-type profile. The fraction of N profile shots for the other pressures averages around 70%. Within a small range of pressures as well as over the whole range of pressures the N-type profile (which have consistently good SXR yields) is clearly similar and distinctly different from the poor shots, which have much lower yields.

There are several features of agreement between the computed and measured yield curves. The peak values are similar at 2.5 J and the shape of the yield curve versus pressure is similar when we compare the measured with the computed curves. The measured peak is, however, flat topped and occurs in a narrow range between 2 and 2.5 torr while the computed yield peak is at a higher value close to 3 torr. The computed yield profile is also significantly narrower than the measured yield profile.

IV. Conclusion

With the help of a template, we have identified how the measured SXR pulse history correlates with the modeled dynamics whenever the PF emits characteristic neon line SXR efficiently in normal N operation. The distinctive feature is that the characteristic neon line SXR is emitted in the first pulse at a moment of time coinciding with the computed pinch phase followed by two to three other similarly shaped pulses of mainly harder SXR. We also looked at the SXR yield time profiles of the nonnormal shots including the conditioning shots.

After one or two conditioning shots, some 75% of the shots are efficient normal N shots over a relatively wide range of operation from 1–4 torr. The point of operation of 2 torr is identified as particularly reproducible in its normal N profile with six out of six shots in one series having the efficient N profile and an overall count of 90%. Moreover, the graph of neon SXR yield versus pressure obtained from the model code broadly agrees with the measured neon SXR yield. These results justify our conclusion that when the INTI PF is within an efficient range of operation the pinch temperature has the suitable temperature to reproducibly and efficiently emit characteristic neon SXR followed by harder XR in a temporal sequence which is identified as normal N. Moreover, this sequence of characteristic neon SXR and harder XR pulses is well correlated to the modeled dynamics; although the results also show the need to refine the model to extend the radiative phase to start before the pinch phase.

References

[1] S. Lee, (2013). *Radiative Dense Plasma Focus Computation Package: RADPF* [Online]. Available: http://www.plasmafocus.net/IPFS/modelpackage/File1RADPF.htm

[2] M. Akel, S. Al-Hawat, S. H. Saw, and S. Lee, "Numerical experiments on oxygen soft X-ray emissions from low energy plasma focus using Lee model," *J. Fusion Energy*, vol. 29, no. 3, pp. 223–231, 2010.

[3] S. H. Saw, P. C. K. Lee, R. S. Rawat, and S. Lee, "Optimizing UNU/ICTP PFF for neon operation," *IEEE Trans. Plasma Sci.*, vol. 37, no. 7, pp. 1276–1282, Jul. 2009.

[4] S. Lee, P. Lee, S. H. Saw, and R. S. Rawat, "Numerical experiments on plasma focus pinch current limitation," *Plasma Phys. Control Fusion*, vol. 50, no. 6, p. 065012, 2008.

[5] S. Lee and S. H. Saw, "Pinch current limitation effect in plasma focus," *Appl. Phys. Lett.*, vol. 92, no. 2, pp. 021503-1–021503-3, 2008.

[6] S. Lee, "Neutron yield saturation in plasma focus: A fundamental cause," *Appl. Phys. Lett.*, vol. 95, no. 15, pp. 151503-1–151503-3, 2009.

[7] S. Lee, R. S. Rawat, P. Lee, and S. H. Saw, "Soft X-ray yield from NX_2 plasma focus," *J. Appl. Phys.*, vol. 106, no. 2, pp. 023309-1–023309-6, 2009.

[8] S. Lee, S. H. Saw, P. C. K. Lee, R. S. Rawat, and H. Schmidt , "Computing plasma focus pinch current from total current measurement," *Appl. Phys. Lett.*, vol. 92, no. 11, pp. 111501-1–111501-3, 2008

[9] S. Lee and S. H. Saw, "Neutron scaling laws from numerical experiments," *J. Fusion Energy*, vol. 27, no. 4, pp. 292–295, 2008.

[10] S. Lee, "Current and neutron scaling for megajoule plasma focus machines," *Plasma Phys. Control Fusion*, vol. 50, no. 10, p. 105005, 2008.

[11] S. Lee, S. H. Saw, P. Lee, and R. S. Rawat, "Numerical experiments on plasma focus neon soft X-ray scaling," *Plasma Phys. Control. Fusion*, vol. 51, no. 10, p. 105013, 2009.

[12] S. Lee, S. H. Saw, A. E. Abdou, and H. Torreblanca, "Characterizing plasma focus devices-Role of the static inductance-instability phase fitted by anomalous resistances," *J. Fusion Energy*, vol. 30, no. 4, pp. 277–282, 2011.

[13] S. Lee, S. H. Saw, R. S. Rawat, P. Lee, A. Talebitaher, A. E. Abdou, P. L. Chong, F. R. A. Singh, D. Wong, and K. Devi, "Correlation of soft x-ray pulses with modeled dynamics of the plasma focus," *IEEE Trans. Plasma Sci.*, vol. 39, no. 11, pp. 3196–3202, Nov. 2011.

[14] S. Lee, T. Y. Tou, S. P. Moo, M. A. Eissa, A. V. Gholap, K. H. Kwek, S. Mulyodrono, A. J. Smith, S. W. Usada, and M. Zakaullah, "A simple facility for the teaching of plasma dynamics and plasma nuclear fusion," *Amer. J.*, vol. 56, no. 1, pp. 62–68, 1988.

[15] S. Lee, S. H. Saw, R. S. Rawat, P. Lee, R. Verma, A. Talebitaher, S. M. Hassan, A. E. Abdou, M. Ismail, A. Mohamed, H. Torreblanca, S. A. Hawat, M. Akel, P. L. Chong, F. Roy, A. Singh, D. Wong, and K. Devi, "Measurement and processing of fast pulsed discharge current in plasma focus machines," *J. Fusion Energy*, vol. 31, pp. 198–204, Jan. 2012.

[16] W. Wang, A. Patran, S. Lee, and P. Lee, "Simple, effective multichannel pin diode X-ray spectrometer system," *Single J. Phys.*, vol. 17, no. 1, pp. 1–27, 2001.

[17] D. Wong, A. Patran, T. L. Tan, R. S. Rawat, and P. Lee, "Soft X-ray optimization studies on a dense plasma focus device operated in neon and argon in repetitive mode," *IEEE Trans Plasma Sci.*, vol. 36, no. 6, pp. 22–67, Dec. 2004.

[18] M. Liu, "Soft X-rays from compact plasma focus," Ph.D. dissertation, School Sci., Nanyang Technol. Univ., Singapore, 1996.

[19] G. X. Zhang, "Plasma soft X-ray source for microelectronich lithography," Ph.D. dissertation, School Sci., Nanyang Technol. Univ., Singapore, 1999.

[20] A. G. Michette and C. J. Buckley, *X-ray Science and Technology*. Bristol, U.K.: Inst. Phys. Publishing, 1993.

[21] B. L. Henke, E. M. Gullikson, and J. C. Davis, "X-ray interactions: Photoabsorption, scattering, transmission, and reflection at E = 50–30, 000 eV, Z = 1–92," *Atmos. Data Nuclear Data Tables*, vol. 54, no. 2, pp. 181–342, Jul. 1993.

[22] S. H. Saw, S. Lee, F. Roy, P. L. Chong, V. Vengadeswaran, A. S. M. Sidik, Y. W. Leong, and A. Singh, "In situ determination of the static inductance and resistance of a plasma focus capacitor bank," *Rev. Sci. Instrum.*, vol. 81, no. 5, p. 053505, May 2010.

[23] A. Bernard, H. Bruzzone, P. Choi, H. Chuaqui, V. Gribkov, J. Herrera, K. Hirano, A. Krej, S. Lee, C. Luo, F. Mezzetti, M. Sadowski, H. Schmidt, K. Ware, C. S. Wong, and V. Zoita, "Scientific status of plasma focus research," *J. Moscow Phys. Soc.*, vol. 8, pp. 93–170, Nov. 1998.

Sor Heoh Saw received the B.Sc. (Hons.) and Ph.D. degrees in physics from the University of Malaya, Kuala Lumpur, Malaysia, in 1985 and 1991, respectively, and the M.A. degree in educational management from the University of Nottingham, Nottingham, U.K., in 1997.

She is a Professor and the Pro Vice-Chancellor for Education Quality and Innovation with INTI International University, Nilai, Malaysia, and is the Director of the Centre for Plasma Research. She is a Co-Director with the Institute of Plasma Focus Studies, Melbourne, Australia, the Designated Delegate of INTI IU, and elected Vice-President with Asian African Association for Plasma Training from 2012 to 2016. Her current research interests include plasma physics and innovation in education.

Dr. Saw was conferred Honorary Membership of Turkish Science and Research Foundation TUBAV in 2009.

Rajdeep Singh Rawat received the B.Sc. (Hons.), M.Sc., and Ph.D. degrees from the University of Delhi, Delhi, India, in 1985, 1987, and 1994, respectively.

He is currently an Associate Professor with the National Institute of Education, Nanyang Technological University, Singapore. He is a President of Asian African Association for Plasma Training and Hon Secretary of Institute of Physics, Singapore. He has authored 136 research papers in journals of international repute and over 63 research papers in conference proceedings. His current research interests include the development of repetitive miniature plasma focus device as portable neutron source, charged particle, and radiation emission from focus devices for nano-phase material synthesis, ion-implantations and lithography applications, and magnetic nanoparticles/nanocomposites and dilute magnetic semiconductor thin films of transition metal doped ZnO using pulsed laser depositions.

Paul Lee received the B.Sc. (Hons.) and Ph.D. degrees from the University of London, London, U.K., in 1992 and 1996, respectively, and the PGDipTHE degree from Nanyang Technological University, Singapore, in 1999.

He is currently an Associate Professor with Nanyang Technological University. He was a Visiting Associate Professor with the University of Washington, Seattle, WA, USA, and Technological Educational Institute, Crete, Greece, in 2007. His current research interests include plasma physics, materials science, and physics education.

Alireza Talebitaher received the B.Sc. degree in electrical and electronic engineering from Amirkabir University, Tehran, Iran, in 1994 and the Ph.D. degree in experimental plasma physics from the National Institute of Education (NIE), Nanyang Technological University, Singapore, in 2013.

He was with the Van de Graaff Laboratory, Fusion Research Center and Plasma Physics Research Center, Tehran, in 1994, as a Staff Engineer and an Electronics Laboratory Instructor until 2008 when he joined NIE, where he is currently a Research Fellow. His current research interests include coded aperture imaging technique for investigation of spatial distribution of fusion source in plasma focus devices.

Dr. Talebitaher is a member of the Institute of Physics, Singapore.

Ali E. Abdou received the B.S. degree in nuclear engineering from Alexandria University, Alexandria, Egypt, the M.S. degree in nuclear engineering, the M.S. degree in computational sciences, and the Ph.D. degree in nuclear engineering from the University of Wisconsin Madison, Madison, WI, USA, in 1992, 2002, 2003, and 2005, respectively.

He has over 15 years of experience in the nuclear science and engineering fields. He participated in the design, preoperation, inauguration, and operation of Egypt's second test and research nuclear reactor ETRR-2 from 1994 to 1999. He is a Licensed Radiation Protection and Health Physicist from Argentinean ENRN and Egyptian NRC in 1996 and 1997, respectively. From 2005 to 2009, he was a Senior Process Development Engineer with Portland Technology Development, Intel Corporation, in the area of plasma etching and semiconductor nanofabrication. He was responsible for the process development of shallow trench isolation for 65, 45, and 32 nm nodes. He is widely expertised in plasma processing techniques used in the fabrication and characterization of semiconductor nano/microstructures. In 2009, he was with the Department of Mechanical and Nuclear Engineering, Kansas State University, Manhattan, KS, USA, as an Assistant Professor of nuclear engineering. He is currently an Associate Professor with the Zewail City of Science and Technology, Zewail, Egypt. He has authored or co-authored over 48 research publications. His current research interests include the development of nanosecond compact multiradiation sources based on the dense plasma focus, the research and development of plasma etching in semiconductor nanofabrication, optical emission spectroscopy, and X-ray emission from plasmas.

Perk Lin Chong received the B.Eng. degree from the University of Liverpool, Liverpool, U.K., in 2000, and the Ph.D. degree from the University of Birmingham, Birmingham, U.K., in 2006.

He is currently a Senior Lecturer with Inti International University, Nilai, Malaysia, and is a member of The Institution of Engineers, Malaysia. His current research interests include numerical computation of plasma focus.

Dr. Chong was a Co-Chair of Seminar on Plasma Focus Experiments (SPFE) in 2010, Secretariat on (SPFE) in 2011, Technical Chair of International Conference on Recent and Emerging Advanced Technologies in Engineering in 2009, Technical Committee (Mechanical Division) of International Conference on CAD/CAM, Robotics and Factories of the Future (CARs & FOF) in 2011, and Reviewer of INTI Journal.

Federico A. Roy, Jr. (M'09) received the B.Sc. degree in electrical engineering from Feati University, Manila, Philippines, in 1982, and the master's degree in electrical engineering from Universiti Tenaga Nasional, Selangor, Malaysia, in 2004. He is currently pursuing the Ph.D. degree in applied physics with Inti International University Malaysia, Nilai, Malaysia.

He is currently a Senior Lecturer with the Faculty of Engineering and Information Technology, Inti International University Malaysia. His current research interests include soft X-ray (plasma focus machine), power systems, and teaching and learning.

Jalil Ali received the Ph.D. degree in plasma physics from Universiti Teknologi Malaysia (UTM), Skudai, Malaysia, in 1990.

He is a Professor of photonics with the Institute of Advanced Photonics Science, Nanotechnology Research Alliance and the Physics Department, UTM and a Visiting Professor with King Mongkut's Institute Technology Ladkrabang, Bangkok, Thailand. From 1987 to 2010, he had held numerous faculty and research positions, including the Dean/Director, Bureau of Innovation, and Consultancy. He was instrumental in establishing and forging University-Industry collaboration in Malaysia. He is currently the Head of Nanophotonics Research Group, UTM, and supervising 20 national/international Ph.D. students as the main supervisor in the field of nanophotonics and plasma focus. His current research interests include photonics, optical solitons, fiber couplers, nanowaveguides, and plasma focus devices.

Dr. Ali is a member of OSA, SPIE, and the Malaysian Institute of Physics. He was awarded the Technology Asean Business Review Award for excellence in government delivery services (Innovation), UTM, in 2008. He is an Editorial Member for a number of journals/special issues such as *Nanosciences and Nanotechnology: An International Journal (NIJ)* and an Editorial Board of *Journal of Biosensor and Bioelectronics-Special Issue on "Biosensors and Bioelectronics On-Chip*.

Sing Lee received the B.Sc. and M.Sc. degrees from the University of Malaya (UM), Kuala Lumpur, Malaysia, in 1964 and 1966, respectively, and the Ph.D. degree from Australian National University, Canberra, Australia, in 1970.

He was a Professor of applied physics and headed research groups in Plasma and Pulse Technology and the Physics Department at UM and was the Head, Division of Physics and Head Academic Group of Natural Sciences with Nanyang Technological University, National Institute of Education, Singapore.

Dr. Lee was an Alexander von Humboldt Fellow from 1975 to 1976 at Kernforschunglange, Juelich, West Germany, Commonwealth Academic Staff Fellow from 1981 to 1982 at Imperial College, London, U.K., a Visiting Professor, and United Nations University Special Fellow from 1986 to 1987 at Flinders University, Bedford Park, South Australia. He was a Founder President of Asian African Association for Plasma Training (AAAPT), an Associate Director of the AAAPT Research and Training Centre at Institute of Physics, Academia Sinica, Beijing, Far Eastern Representative and a Director of Plasma Physics College of the International Centre for Theoretical Physics, Trieste, and an Ardent Advocate and implementer of south-south technology creation and transfer in plasma fusion, laser and pulse technology. He is a Chartered Physicist and a fellow of Institute of Physics, U.K., a Life and Hon Fellow of Institute of Physics Malaysia, Life Fellow of Singapore Institute of Physics, and the Samahang Pisika ng Pilipinas and Hon Member of the Turkish Science and Research Foundation TUBAV. He is a Founding Director of Institute for Plasma Focus Studies, Melbourne, an Adjunct Professor (Hon) of INTI International University, Nilai, Malaysia, and Emeritus Professor of UM, Malaysia.